Electronic Supplementary Material (EIS) for ChemComm.

This journal is © The Royal Society of Chemistry 2025

Supporting Information

$NiMoO_4$ decorated $Co(OH)_2$ nanosheets as an efficient bifunctional electrocatalyst for urea-assisted water splitting

Feng Jing,[*ab] Zhen Liu,[bc] Sihan Fu,[a] Bo Cheng,[c] Zhiyi Wang,[c] Kangwen Qiu[*ab]

[a] College of Energy Engineering, Huanghuai University, Zhumadian 463000, Henan Provinve, P. R. China

[b] Henan Key Laboratory of Smart Lighting, Huanghuai University, Zhumadian 463000, Henan Provinve, P. R. China

[c] College of Information Engineering, Huanghuai University, Zhumadian 463000, Henan Provinve, P. R. China

*Corresponding author E-mail: mpcjfeng@163.com (Feng Jing)

Experimental

Chemicals and materials

$Ni(CH_3COO)_2 \bullet 4H_2O$, $Na_2MoO_4 \bullet 2H_2O$ and urea were purchased from Sinopharm Chemical Reagent Co., Ltd. $Co(NO_3)_2 \bullet 6H_2O$ was provided from Shanghai Aladdin Biochemical Technology Co., Ltd. NH_4F was provided from Shanghai Macklin Biochemical Technology Co., Ltd. Nickel foam (NF) was purchased from Suzhou Keshenghe Metal Materials Co., LTD. The deionized water was purified and collected by a Youpu ultrapure water purification system.

Sample synthesis

Synthesis of $Co(OH)_2$/NF

A piece of NF (1 × 2 cm) was treated in immersed in 1 M HCl for 30 min to remove the nickel oxides on the surface and then sequentially washed with deionized water and ethanol three times. Firstly, 9 mmol $Co(NO3)_2$, 30 mmol urea and 16 mmol NH_4F were added in deionized water and pre-treated NF was added into above solution. Secondly, after heating at 120 ℃ for 6 h， $Co(OH)_2$/NF was obtained.

Synthesis of $Co(OH)_2/NiMoO_4$/NF

The $Co(OH)_2$/NF was immersed mixed solution contained 0.025 mmol $Ni(CH_3COO)_2$， 0.004 mmol Na_2MoO_4 and 0.1 mmol urea, which was heated for 10 h at 160 ℃. The hierarchica $Co(OH)_2/NiMoO_4$/NF heterostructure was thus prepared with cooling to room temperature. To determine the optimal growth duration of $NiMoO_4$, we prepared three samples under identical conditions for durations of 5 hours, 15 hours, and 20 hours, respectively. These samples were designated as $Co(OH)_2/NiMoO_4$-5/NF, $Co(OH)_2/NiMoO_4$-15/NF, and $Co(OH)_2/NiMoO_4$-20/NF. Furthermore, unless otherwise specified, all references to $Co(OH)_2/NiMoO_4$/NF in this work correspond to samples prepared with a $NiMoO_4$ growth time of 10 hours.

Materials characterization

The morphologies of as-prepared electrodes were study by field-emission scanning electron microscope (SEM, Nova NanoSEM 450) and transmission electron microscopy (TEM, FEI Talos F200S). The diffractometer of Philips PW-1830 equipped with a Cu Kα radiation (λ = 0.15406 nm) is used to record X-ray powder diffraction (XRD) patterns of obtained electrodes. X-ray photoelectron spectroscopy (XPS) are measured by Perkin-Elmer model PHI 5600 XPS system with an Al Kα X-ray source (1486.6 eV).

Electrochemical Characterizations

All the electrochemical performances were tested with the CHI760E workstation (CH Instruments, Inc., Shanghai) with obtained catalysts as working electrode. Linear sweep voltammetry (LSV) measurements were carried out at a scan rate of 5 mV s^{-1}. Unless otherwise specified, each potential was *iR*-corrected. Cycle voltammetry (CV) curves were tested to estimate the electrochemically active surface with various scan rates and 20 continuous sweep cycles were performed to ensure consistency. Electrochemical impedance spectroscopy (EIS) analysis was carried out at the frequency range of 10 mHz-100 kHz with. The long-term (48 h) stability tests was performed using chronopotentiometric measurements with a constant current density of 10 mA cm^{-2}.

DFT Calculations

The Quantum Espresso [1] based on the projector augmented wave (PAW) method [2] was implemented in computational work. Perdew-Burke-Ernzerhof (PBE) generalized gradient approximation (GGA) [3] and DFT-D3 method [4] were employed to describe the exchange-correlation functional and van der Waals forces. The Monkhorst-Pack k-point [5] of 12 × 10 × 1 grids and a kinetic energy cut-off of 50 Ry were used in the computations, with the energy and force convergence criteria set to 10-4 Ry/Bohr and 10-6 Ry, respectively. A 25 Å vacuum layer in the stack direction was introduced to avoid interaction between neighboring periodic structures. The heterostructure was simulated with a bilayer-thick of $Co(OH)_2$ and tetralayer-thick of $NiMoO_4$.

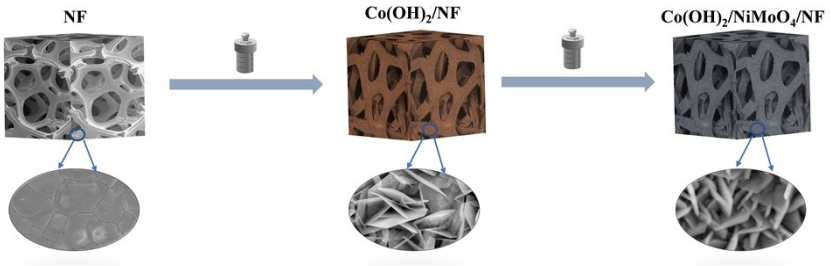

Fig. S1 Schematic illustration for preparing $Co(OH)_2/NiMoO_4/NF$.

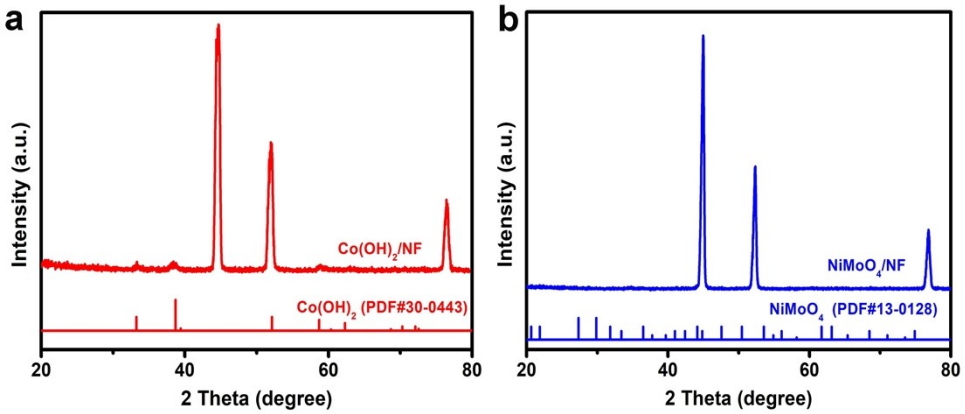

Fig. S2 XRD diffraction pattern of $Co(OH)_2/NF$ (**a**) and $NiMoO_4/NF$ (**b**).

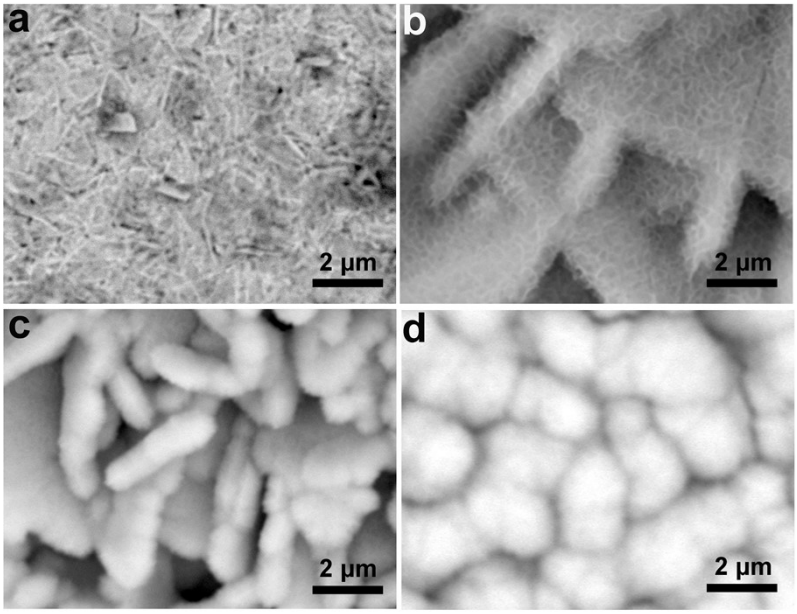

Fig. S3 SEM image of the $Co(OH)_2/NiMoO_4$-5/NF(**a**), $Co(OH)_2/NiMoO_4$/NF(**b**), $Co(OH)_2/NiMoO_4$-15/NF(**c**) and $Co(OH)_2/NiMoO_4$-20/NF (**d**).

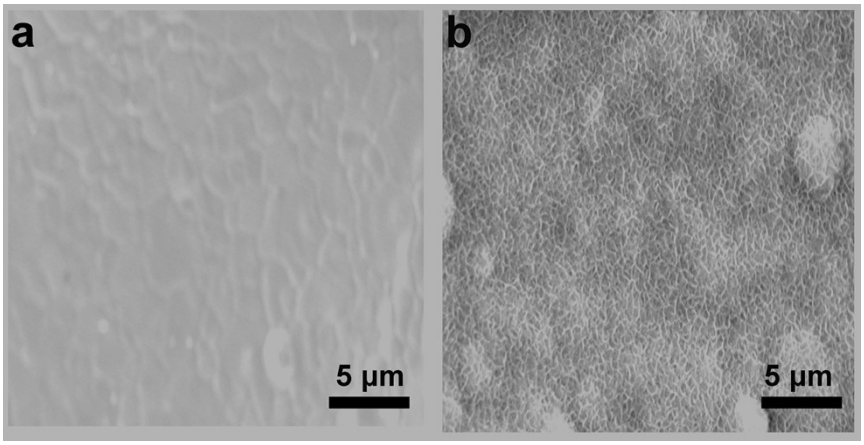

Fig. S4 SEM images of NF (**a**) and $NiMoO_4$/NF (**b**)

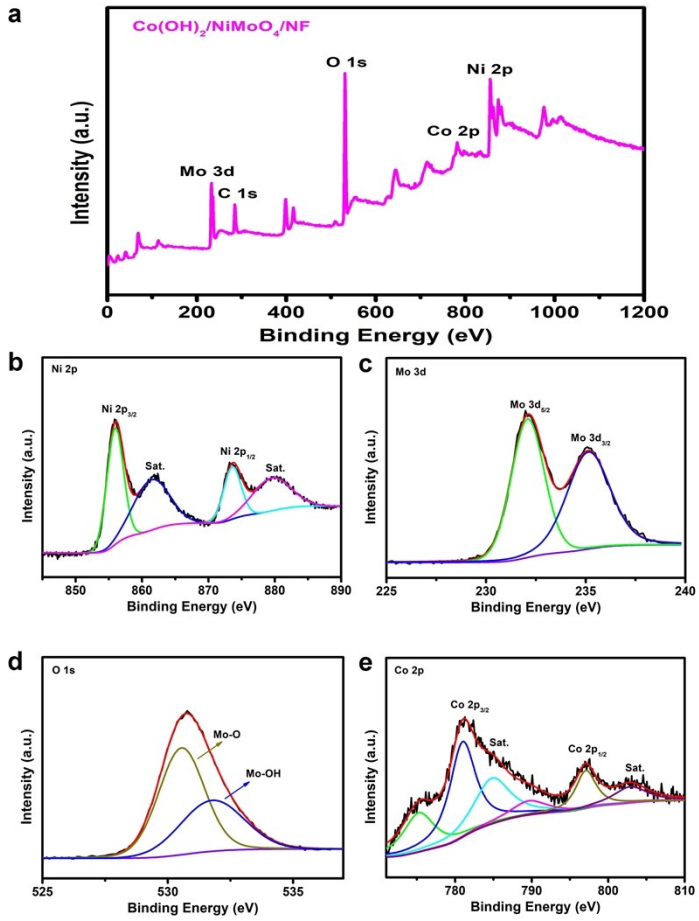

Fig. S5 XPS spectra of (**a**) wide scan spectrum, (**b**) Ni 2p, (**c**) Mo 3d, (**d**) O 1s, and (**e**) Co 2p for $Co(OH)_2/NiMoO_4/NF$.

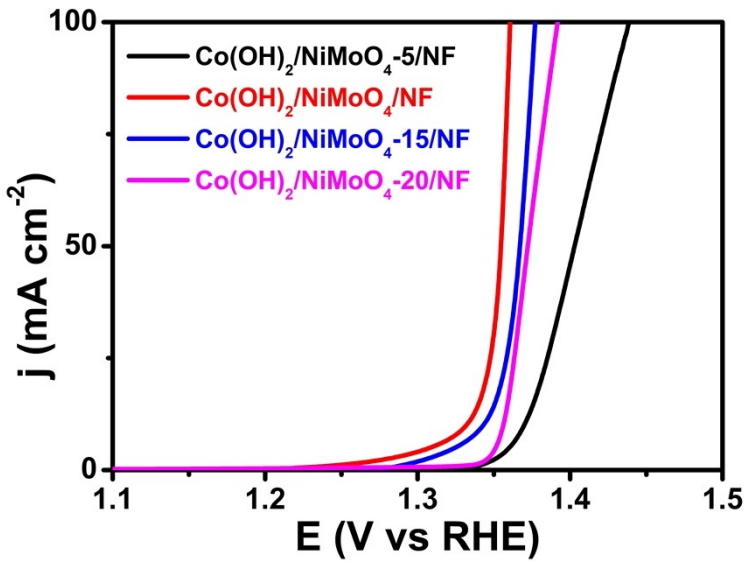

Fig. S6 LSV curves of the $Co(OH)_2/NiMoO_4$-5/NF, $Co(OH)_2/NiMoO_4$/NF, $Co(OH)_2/NiMoO_4$-15/NF and $Co(OH)_2/NiMoO_4$-20/NF for the UOR in 1.0 M KOH containing 0.5 M urea.

Table S1. Comparison of the impacts of the growth time of $NiMoO_4$, thickness of the hybrid nanosheet and loading contents of the two components on UOR performance.

Catalyst	Growth time of $NiMoO_4$	Thickness of the hybrid nanosheet	Ratio of mass (m_{NiMoO4}:$m_{Co(OH)2}$)	Voltage for UOR at j = 10 mA cm^{-2}
$Co(OH)_2/NiMoO_4$-5/NF	5	-	-	1.370 V
$Co(OH)_2/NiMoO_4$/NF	**10**	**~1.178 μm**	**~0.50:1**	**1.332 V**
$Co(OH)_2/NiMoO_4$-15/NF	15	~1.172 μm	~0.58:1	1.344 V
$Co(OH)_2/NiMoO_4$-20/NF	20	-	~0.71:1	1.356 V

Table S2. Comparison of UOR performance of $Co(OH)_2/NiMoO_4/NF$ electrode with various well-developed catalysts in 1 M KOH containing 0.5 M urea.

Catalyst	Voltage for UOR at j / (V @ mA cm^{-2})	Tafel slope / (mV dec^{-1})	Ref.
$Co(OH)_2/NiMoO_4/NF$	**1.332@10** **1.361@100**	**25.5**	**This work**
$Ni_{0.75}Fe_{0.25}Se_2/CC$	1.343@10	73	S6
N-Ni-MoO_2/NF	1.351@10	38.69	S7
$Co(OH)_2$/AlOOH/NF-100	1.36@10	58.32	S8
Ni@NCDs	1.38@10	36.7	S9
Co/Zn-Pi@NF	1.40@10	95.8	S10
Co3O4/Ti3C2 MXene	1.40@10	149	R22
NF/CoP@Ni_3S_2	1.379@100	24.7	S11
CF@Ni/Ni_4Mo-5	1.396 V@100	31.4	R11
$CoS_x/Ni(OH)_2$/NF	1.409@100	46.9	R1
hollow NiCoP nanoprisms	1.42@100	59	S12
$CoMoO_4/Co_9S_8$/N	1.50@100	21.79	S13
CoMoO@Co/GF	1.515@100	58.7	S14

Table S3. The fitting parameters from Nyquist plots with Randles circuit for UOR

Parameter / Electrode	UOR	
	R_{ct} / Ω	R_s / Ω
$Co(OH)_2/NiMoO_4/NF$	1.3	1.3
$NiMoO_4$/NF	1.6	1.6
$Co(OH)_2$/NF	2.4	1.9
NF	4.0	1.4

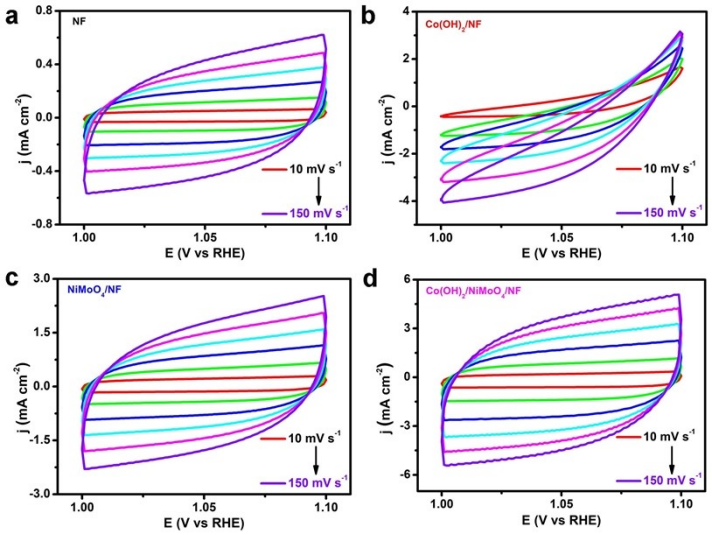

Fig. S7 CV curves of the NF (**a**), $Co(OH)_2$/NF (**b**), $NiMoO_4$/NF (**c**), $Co(OH)_2$/$NiMoO_4$/NF (**d**).

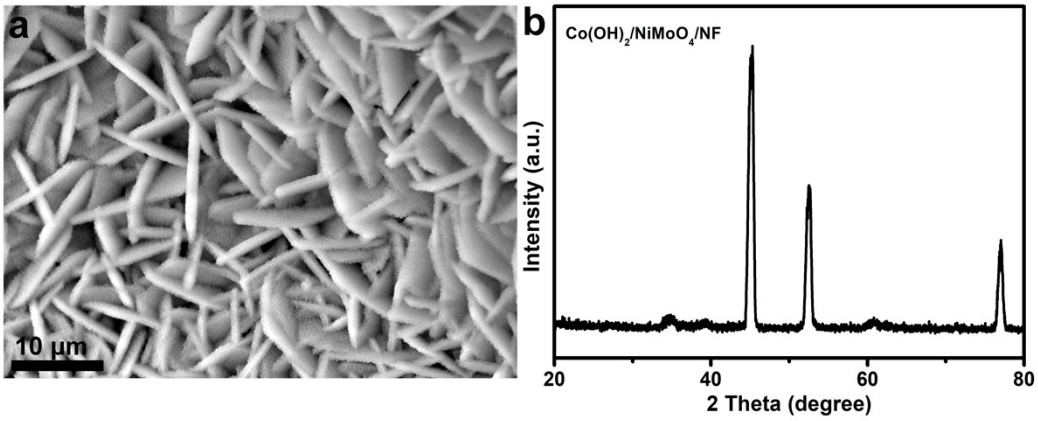

Fig. S8 SEM image (**a**) and XRD pattern (**b**) of $Co(OH)_2$/$NiMoO_4$/NF after the UOR stability.

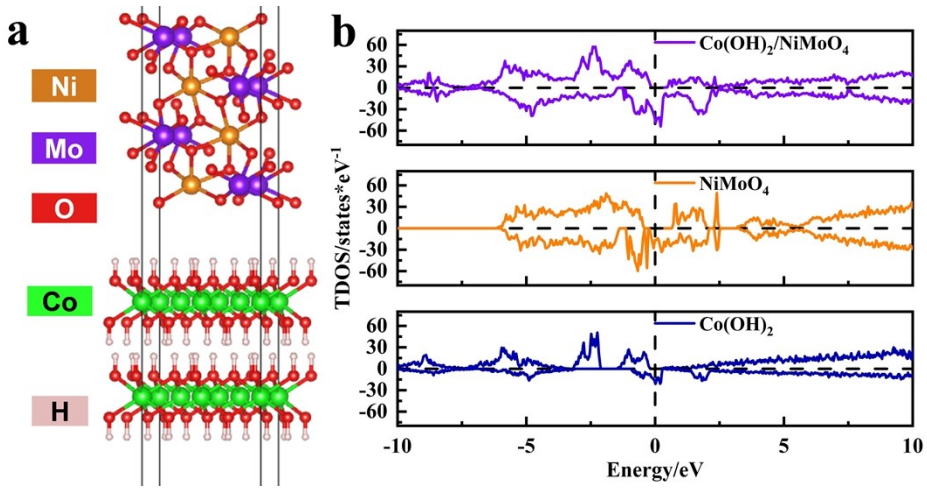

Fig. S9 The crystal structure of $Co(OH)_2/NiMoO_4$ (**a**) and TDOS of $Co(OH)_2/NiMoO_4$, $NiMoO_4$ and $Co(OH)_2$(**b**).

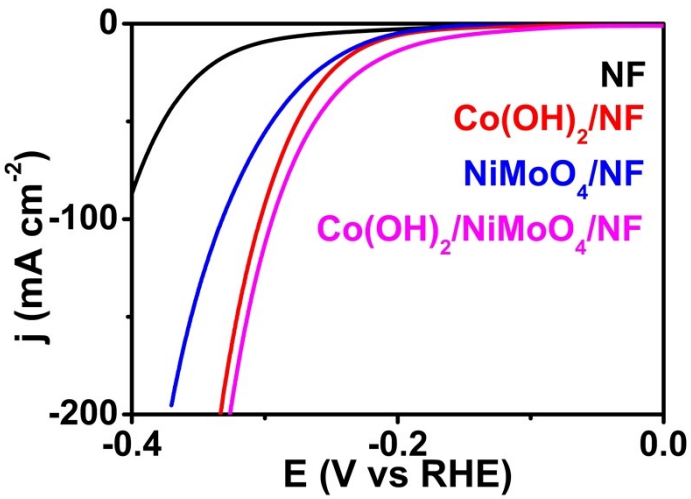

Fig. S10 LSV curves of $Co(OH)_2/NiMoO_4/NF$, $NiMoO_4/NF$, $Co(OH)_2/NF$ and NF for the HER in 1.0 M KOH.

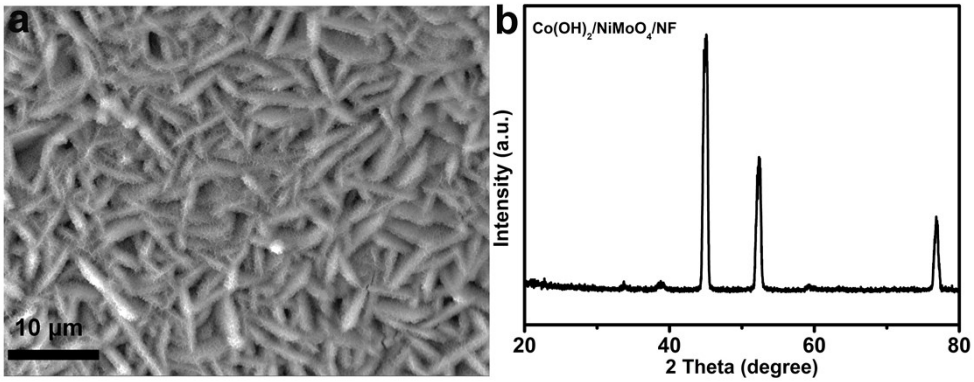

Fig. S11 SEM image (**a**) and XRD pattern (**b**) of $Co(OH)_2/NiMoO_4/NF$ after the HER stability.

Table S4. Comparison of urea electrolysis performances of as-obtained $Co(OH)_2/NiMoO_4/NF$ with recently reported bifunctional catalysts in 1 M KOH containing 0.5 M urea.

Catalyst	Voltage at j = 10 mA cm^{-2}	Ref.
$Co(OH)_2/NiMoO_4/NF$	**1.535 V**	**This work**
Ce-NiVS/NF	1.55 V	S15
$Fe_7Se_8@Fe_2O_3$	1.55 V	S16
Bulk MnO_2	1.55 V	S17
Ni@NCNT	1.56 V	S18
W-Ni_3S_2/NiS	1.569 V	S19
Co-Ni_5P_4-NiCoOH	1.57 V	S20
$MnO_2/MnCo_2O_4$/N	1.58 V	S21
FQD/CoNi LDH/N	1.59 V	S22
HC-NiMoS/T	1.59 V	S23
$Ni(OH)_2$NS@NW/NF	1.68 V	S24

References

S1 P. Giannozzi, S. Baroni, N. Bonini, M. Calandra, R. Car, C. Cavazzoni, D. Ceresoli, G. L. Chiarotti, M. Cococcioni, I. Dabo, A. D. Corso, S. D. Gironcoli, S. Fabris, G. Fratesi, R. Gebauer, U. Gerstmann, C. Gougoussis, A. Kokalj, M. Lazzeri, L. M-. Samos, N. Marzari, F. Mauri, R. Mazzarello, S. Paolini, A. Pasquarello, L. Paulatto, C. Sbraccia, S. Scandolo, G. Sclauzero, A. P. Seitsonen, A. Smogunov, P. Umari and R. M. Wentzcovitch, *J. Phys.: Condens. Matter*, 2009, **21**, 395502.

S2 G. Kresse and and D. Joubert, *Phys. Rev. B*, 1999, **59**, 1758.

S3 J. P. Perdew, K. Burke and M. Ernzerhof, *Phys. Rev. Lett.*, 1997, **78**, 1396.

S4 S. Grimme, J. Antony, S. Ehrlich and H. Krieg, *J. Chem. Phys.*, 2010, **132**, 154104.

S5 H. J. Monkhorst and J. D. Pack, *Phys. Rev. B*, 1976, **13**, 518.

S6 M. Zhu, P. C. Tang, X. Y. Li, M. Zhao, L. N. Liu, W. X. Tang, Z. H. Xu, G. H. Dong, M. R. Yang and Z. C. Shi, *Int. J. Hydrogen Energy*, 2025, **102**, 626.

S7 G. F. Qian, T. Lu, Y. P. Wang, H. T. Xu, X. Y. Cao, Z. H. Xie, C. Z. Chen and D. Y. Min, *Chem. Eng. J.*, 2024, **480**, 147993.

S8 M. L. Yan, J. J. Zhang, C. Wang, L. Gao, W. G. Liu, J. H. Zhang, C. Q. Liu, Z. W. Lu, L. J. Yang, C. L. Jiang and Y. Zhao, *J. Colloid Interface Sci.*, 2025, **677**, 1069.

S9 Y. C. Pan, J. C. Zhang, Q. Zhang, X. Chen, Q. Wang, C. C. Li, Z. L. Liu and Q. F. Sun, *Mater. Chem. Front.*, 2023, **7**, 3340.

S10 R. Zhang, Y. J. Wang, X. Y. Gao, D. H. Duan, J. W. Wang and S. B. Liu, *J. Alloys Compd.*, 2024, **1009**, 176818.

S11 D. F. Wen, M. Ye, Y. Xia, W. S. Mai, Z. Q. Zhang, W. T. Zhang, W. D. Peng, W. Hu and L. H. Tian, *Appl. Surf. Sci.*, 2022, **586**, 152736.

S12 X. D. Ding, L. S. Pei, Y. X. Huang, D. Y. Chen and Z. L. Xie, *Small*, 2022, **18**, 2205547.

S13 X. Q. Du, C. R. Huang and X. S. Zhang, *Int. J. Hydrog. Energy.*, 2019, **44**, 19595.

S14 L. Lei, Z. Yin, D. L. Huang, Y. S. Chen, S. Chen and M. Cheng, *J. Colloid. Interface Sci.*, 2022, **612**, 413.

S15 C. Wang, X. R. Wang, X. Q. Du and X. S. Zhang, *Dalton Trans.*, 2023, **52**, 13161.

S16 J. X. Li, X. Q. Du, X. S Zhang and Z. P. Wang, *Int. J. Hydrog. Energy.*, 2022, **47**, 35203.

S17 S. Chen, J. J. Duan, A. Vasileff and S. Z. Qiao, *Angew. Chem. Int. Edit.*, 2016, **55**, 3804.

S18 Q. Zhang, F. MD. Kazim, S. X. Ma, K. G. Qu, M. Li, Y. G. Wang, H. Hu, W. W. Cai and Z. H. Yang, *Appl. Catal. B-Environ.*, 2021, **280**, 119436.

S19 H. Zhao, M. Liu, X. Q. Du and X. S. Zhang, *Dalton Trans.*, 2023, **52**, 8811.

S20 Y. H. Wang, C. Y. Zhang, X. Q. Du and X. S. Zhang, *Dalton Trans.*, 2022, **51**, 14937.

S21 C. L. Xiao, S. N. Li, X. Y. Zhang and D. S. MacFarlane, *J. Mater. Chem. A.*, 2017, **5**, 7825.

S22 Y. Q. Feng, X. Wang, J. F. Huang, P. P. Dong, J. Ji, J. Li, L. Y. Cao, L. L. Feng, P. Jin and C. R. Wang, *Chem. Eng. J.*,2020, **390**, 124525.

S23 X. X. Wang, J. M. Wang, X. P. Sun, S. Wei, L. Cui, W. R. Yang and J. Q. Liu, *Nano Res.*, 2018, **11**, 988.

S24 Z. H. Yue, S. Y. Yao, Y. Z. Li, W. X. Zhu, W. T. Zhang, R. Wang, J. Wang, L. J. Huang, D. Y. Zhao and J. L. Wang, *Electrochim. Acta.*, 2018, **268**, 211.